Separability, Asymptotics, and Applications of the SIR Meta Distribution in Cellular Networks

Ke Feng, *Student Member, IEEE*, and Martin Haenggi, *Fellow, IEEE*

***Abstract*—The signal-to-interference-ratio (SIR) meta distribution (MD) characterizes the link performance in interference-limited wireless networks: it evaluates the fraction of links that achieve an SIR threshold θ with a reliability above x. In this work, we show that in Poisson networks, for any independent fading and power-law path loss with exponent α, the SIR MD can be expressed as the product of $\theta^{-2/\alpha}$ and a function of x when (θ, x) is in the so-called "separable region". We show by simulation that the separable form serves as a good approximation of the SIR MD in Ginibre and triangular lattice networks when θ is chosen large enough. Given the quest for ultra-reliable transmission, we study the asymptotics of the SIR MD as $x \to 1$ for general cellular networks with Rayleigh fading. Finally, we apply our results to characterize the distribution of the link rate, where each link transmits with a rate satisfying a given reliability x, and the asymptotic distribution of the local delay, defined as the number of transmissions needed for a message to be received successfully.**

***Index Terms*—Cellular networks, meta distribution, Poisson point process, separability, stochastic geometry, local delay**

I. Introduction

A. Motivation

The signal propagation in wireless networks is subject to small-scale fading and large-scale path loss, and the signal-to-interference-ratio (SIR) is a key quantity in interference-limited scenarios. Consider a cellular network where base station (BS) locations are modeled using a stationary and ergodic point process $\Phi \subset \mathbb{R}^2$ and the typical user located at the origin[1]. Let $x \in \Phi$ be the serving BS and $\Phi \setminus \{x\}$ be the set of interfering BSs. The SIR at the typical user is

$$\mathrm{SIR} \triangleq \frac{h_x \|x\|^{-\alpha}}{\sum_{y \in \Phi \setminus \{x\}} h_y \|y\|^{-\alpha}}, \tag{1}$$

where h_x denotes the fading associated with BS x and $\|\cdot\|^{-\alpha}$ denotes the path loss with exponent α. Given the BS locations, the SIR received at the typical user is subject to the randomness of small-scale fading only. In this case, the reliability of the link with respect to θ is defined as

$$P_{\mathrm{s}}(\theta) \triangleq \mathbb{P}(\mathrm{SIR} > \theta \mid \Phi), \quad \theta > 0, \tag{2}$$

which is referred to as the conditional success probability interchangeably [1] since it evaluates the probability of success conditioned on the BS point process. The distribution of $P_{\mathrm{s}}(\theta)$ depends on the distribution of Φ. It is vital to study the distribution of the link reliability, which answers "what is the fraction of links in the network that achieve an SIR threshold θ with a reliability above x?" Consequently, the SIR meta distribution (MD) is defined as [1]

$$\bar{F}_{P_{\mathrm{s}}}(\theta, x) \triangleq \mathbb{P}(P_{\mathrm{s}}(\theta) > x), \quad x \in [0, 1], \tag{3}$$

which is the CCDF of the conditional success probability. For any ergodic BS point process, the SIR MD can be interpreted as the fraction of links that achieves θ with reliability higher than x in any realization of the network. Generally, $\bar{F}_{P_{\mathrm{s}}}(\theta, x)$ monotonically decreases with θ and x, and $\bar{F}_{P_{\mathrm{s}}}(\theta, 1) = 0$.

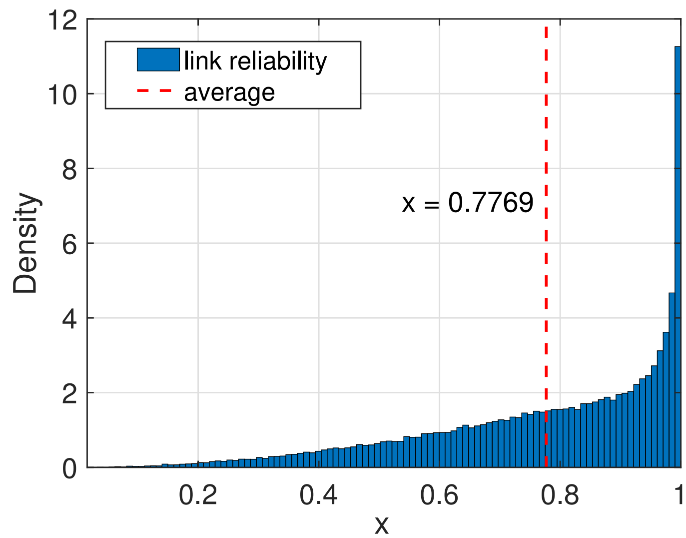

Fig. 1. Histogram of $P_{\mathrm{s}}(\theta)$ for $\theta = -5$ dB in a Poisson cellular network with Rayleigh fading and power-law path loss with $\alpha = 4$. The mean reliability $x = 0.7769$, and approximately 58.2% of the links achieve $\theta = -5$ dB with reliability above $x = 0.7769$.

Fig. 1 shows the histogram of the conditional success probability for $\theta = -5$ dB in a Poisson network with Rayleigh fading and power-law path loss with exponent $\alpha = 4$. In this example, approximately 58.2% links achieve $\theta = -5$ dB with a reliability above $x = 0.7769$, which is the mean success probability in this example. The (mean) success probability is a simpler and more extensively explored metric in the literature. By definition,

$$p_{\mathrm{s}}(\theta) \equiv \mathbb{E}[P_{\mathrm{s}}(\theta)]. \tag{4}$$

The SIR MD is a fine-grained metric of the link-level performance in the network. However, only a few analytical properties are available even for the most tractable model, the Poisson point process (PPP). As such, the analytical properties of the SIR MD and their applications are the subjects of study in this work.

[1]By the stationarity of the point process, we assume that the typical user is located at the origin without loss of generality.

B. Prior Work

As a critical metric for network performance, the SIR MD for cellular networks with BS cooperation is analyzed in [2], with non-orthogonal multiple access (NOMA) in [3], with offloading in [4], [5], and with power control in [6]. [7] studies the MD in the Poisson typical cell while [8], [9] provide approximations of the MD for non-Poisson cellular networks. The MD for Poisson bipolar networks is studied in [10] as a basis for the spatial outage capacity. [11] studies the MD in networks with bipartite Euclidean matchings. Most of the work mentioned above evaluate the MD based on simulations or approximations due to the lack of efficient analytical methods. And numerical methods are proposed in [12], [13] to calculate the MD based on the moments of the conditional success probability, which are often more tractable.

The moments of the conditional success probability in Poisson networks and an exact integral expression for the MD are given in [1]. The authors in [8] study the asymptotics of the moments as $\theta \to 0$ for general networks. They propose to approximate the SIR MD for non-Poisson networks using the shifted version of the MD for Poisson networks. However, only Rayleigh fading is studied in [1], [8]. Relevant to this work, [14, Cor. 2] puts forth an idea of characterizing the SIR MD in Poisson networks by conditioning on the distance ratio of the nearest two BSs, which applies to general fading models as will be shown in this work.

The SIR MD can be interpreted as the distribution of the link rate, given that the transmission rate of each link is adjusted to achieve a target reliability x [15]. Given the quest for ultra-reliable transmission in 5G and beyond communication systems [16], the link-level reliability is expected to be higher than $1 - 10^{-5}$. It is thus critical to explore the asymptotic behavior of the SIR MD in cellular networks as $x \to 1$, which has not been studied so far. Asymptotic analyses of the (mean) success probability show that, for general 2D stationary point processes under general iid fading and power-law path loss, $p_{\rm s}(\theta) = \Theta(\theta^{-\delta})$ as $\theta \to \infty$ with $\delta \triangleq 2/\alpha$ [17]–[20]. In comparison, this work studies the asymptotics of the MD as $\theta \to \infty$ and as $x \to 1$. And we exploit the connection between the link reliability, rate, and local delay [21] in the context of the SIR MD.

C. Contributions

- We show that in Poisson networks with power-law path loss, the SIR MD for any independent fading, either identically or non-identically distributed, can be expressed as the product of $\theta^{-\delta}$ and a function of only x for $(\theta, x) \in \mathcal{D}$, where $\mathcal{D}$ is referred to as the *separable region*. In particular, we show that
$$\bar{F}_{P_{\rm s}}(\theta, x) = g(x)\theta^{-\delta}, \quad (\theta, x) \in \mathcal{D}, \tag{5}$$
where g is strictly monotonically decreasing from 0 to 1, with $g(1) = 0$, and $\mathcal{D}$ is explicitly defined by the fading statistics. (5) is referred to as the *separability of the SIR MD in Poisson networks*.
- We show that $\mathcal{D}$ covers half of the parameter space for any iid fading, and we specify $\mathcal{D}$ for iid Nakagami-m fading. Further, $g(x)$ for two special cases are studied: no fading and Rayleigh fading. For the no fading case, we give the exact expression of $g(x)$. For Rayleigh fading, we provide three approximations of $g(x)$.
- We show by simulation that the SIR MD is well approximated by $g(x)\theta^{-\delta}$ for Ginibre and triangular lattice networks when θ is chosen large enough.
- We study the asymptotics of the SIR MD as $x \to 1$ for all simple point processes with Rayleigh fading, which shows that the effect of the network geometry and Rayleigh fading are essentially separable as $x \to 1$.
- We study the distribution of the link rate and local delay using the SIR MD with a focus on Poisson networks. We show that there is an optimal reliability that maximizes the ergodic rate normalized by the reliability. Further, we give the asymptotic form of the CDF of the local delay in Poisson networks with Rayleigh fading.

II. System Model

A. System Model

We consider independent fading, power-law path loss with exponent $\alpha > 2$ and stationary and ergodic BS point processes. We assume that the typical user (located at the origin o) is always associated with its nearest BS. Let $x_i(o)$ denote the i-th nearest BS to the typical user and h_i the associated fading power, $i \in \mathbb{N}$. The conditional success probability is
$$P_{\rm s}(\theta) = \mathbb{P}\left(\frac{h_1 \|x_1(o)\|^{-\alpha}}{\sum_{i=2}^{\infty} h_i \|x_i(o)\|^{-\alpha}} > \theta \;\middle|\; \Phi \right). \tag{6}$$
It is apparent that only the fading statistics and distance ratios matter in (6). Among the distance ratios $\|x_1(o)\|/\|x_i(o)\|$, $\|x_1(o)\|/\|x_2(o)\|$ has the greatest impact on the link reliability due to the ordering of distances. This observation leads us to rank the link reliability by the *global information* and the *local information*[2].

B. Link Reliability Ranking

1) Global information: The most fine-grained link reliability ranking takes into account the entire network geometry, which we refer to as the "global information". Naturally, for a given $x \in [0, 1]$, the global information-based top-reliability links are those that satisfy $P_{\rm s}(\theta) > x$. The fraction of the top-reliability links is given by the SIR MD.

2) Local information: A coarse characterization of the link reliability is based on the distance ratio $\|x_1(o)\|/\|x_2(o)\|$, which we refer to as the "local information". For a given $\rho \in [0, 1]$, the local information-based top-reliability links are those that satisfy $\|x_1(o)\| \leq \rho\|x_2(o)\|$. The percentage of the top-reliability links depends on the distribution of the distance ratio $\|x_1(o)\|/\|x_2(o)\|$.

Fig. 2a shows the color map of the link reliability in the Voronoi cells for a given realization of a Poisson point process. Fig. 2b shows the locations satisfying $\|x_1(o)\| = \|x_2(o)\|/\sqrt{2}$ underlaid by the reliability color map. From this figure, links satisfying $\|x_1(o)\| \leq \|x_2(o)\|/\sqrt{2}$ have a higher reliability on average.

[2] A similar idea can be found in [22], where the observation of global or nearby interferers is used to predict the probability of successful transmission.

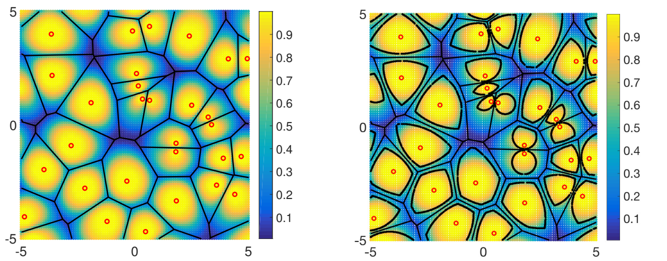

(a) Color map of link reliability.

(b) Color map with black dots representing locations where $\|x_1(o)\| = \|x_2(o)\|/\sqrt{2}$.

Fig. 2. Color maps of the link reliability for $\theta = 1$, $\alpha = 4$ and Rayleigh fading. Red circles denote BS locations generated from a PPP with $\lambda = 1$ and black lines denote the boundary of Voronoi cells.

3) Relation of the two rankings: In general, for any $\rho \in [0, 1]$,

$$\mathbb{P}(P_{\mathrm{s}}(\theta) > x) \geq \mathbb{P}\big(P_{\mathrm{s}}(\theta) > x, \|x_1(o)\| \leq \rho\|x_2(o)\|\big), \quad (7)$$

which is due to the Bayesian theorem. A question of interest is whether there exists a critical $\rho_c < 1$ such that the inequality becomes an equality, *i.e.*,

$$P_{\mathrm{s}}(\theta) > x \quad \Rightarrow \quad \|x_1(o)\|/\|x_2(o)\| \leq \rho_c. \quad (8)$$

In other words, no links with $\|x_1(o)\| > \rho_c\|x_2(o)\|$ can achieve $P_{\mathrm{s}}(\theta) > x$. An immediate conjecture is that (8) holds when either θ or x is large enough, which we will prove in the next section.

III. Separability of the SIR MD

We now study the separability of the SIR MD distribution in Poisson networks. We first present some basic properties of Poisson networks. To simplify the notation, we define $r_i \triangleq \|x_i(o)\|$ and $t_i \triangleq r_i/r_{i+1}$ for $i \in \mathbb{N}$.

A. Basic Properties of the Poisson Point Process

Lemma 1. For a homogeneous Poisson point process in $\mathbb{R}^m$,

$$\mathbb{P}(t_i \leq x) = x^{mi}, \quad x \in [0, 1]. \quad (9)$$

Proof.

$$\begin{aligned}\mathbb{P}(t_i \leq x) &= \mathbb{E}[\mathbb{P}(t_i \leq x \mid r_{i+1})] \\ &= \mathbb{E}[\mathbb{P}(r_i \leq x r_{i+1} \mid r_{i+1})] \\ &\overset{\text{(a)}}{=} x^{mi}.\end{aligned}$$

Step (a) follows from the fact that conditioning on r_{i+1}, the i points $x_1(o), ..., x_i(o)$ are independently and uniform randomly distributed in the m-dimensional ball with radius r_{i+1}. r_i is the maximum distance of the i points and the distance ratio t_i does not depend on the value of r_{i+1} for $i \in \mathbb{N}$. □

Lemma 1 shows that $1/t_i$ is Pareto distributed in Poisson networks. t_i is likely to have a value close to 1 when i is large, which is intuitive since the void probability depends on the volume $c_m(r_i^m/x^m - r_i^m)$, which depends on r_i. Alternatively, we can prove Lemma 1 by conditioning on r_i and using the void probability of the PPP and the distribution of r_i [23].

Lemma 2. For a Poisson point process in $\mathbb{R}^m$, the set of random variables $\{t_i\}_{i\in\mathbb{N}}$ are pairwise independent. Further, $\{t_{m_1}, t_{m_2}, ...t_{m_k}\}$ is independent of $\{t_{n_1}, t_{n_2}, ...t_{n_l}\}$ if $\max(m_1, ...m_k) < \min(n_1, ...n_l)$ or $\min(m_1, ...m_k) > \max(n_1, ...n_l)$.

Proof. We first establish the pairwise independence by showing for $\forall i \neq j,\ i, j \in \mathbb{N}$

$$\mathbb{P}(t_i \leq x, t_j \leq y) = \mathbb{P}(t_i \leq x)\mathbb{P}(t_j \leq y). \quad (10)$$

It is sufficient to prove (10) for two cases: $j = i + 1$ and $j > i + 1$. For $j = i + 1$,

$$\begin{aligned}&\mathbb{P}(t_i \leq x, t_j \leq y) \\ &\quad= \mathbb{E}\Big[\mathbb{P}\Big(\frac{r_i}{r_{i+1}} \leq x, \frac{r_{i+1}}{r_{i+2}} \leq y \;\Big|\; r_{i+1}\Big)\Big] \\ &\quad\overset{\text{(a)}}{=} \mathbb{E}\Big[\mathbb{P}\Big(\frac{r_i}{r_{i+1}} \leq x \;\Big|\; r_{i+1}\Big)\mathbb{P}\Big(\frac{r_{i+1}}{r_{i+2}} \leq y \;\Big|\; r_{i+1}\Big)\Big] \\ &\quad\overset{\text{(b)}}{=} \mathbb{P}\Big(\frac{r_i}{r_{i+1}} \leq x\Big)\mathbb{E}\Big[\mathbb{P}\Big(\frac{r_{i+1}}{r_{i+2}} \leq y \;\Big|\; r_{i+1}\Big)\Big] \\ &\quad= \mathbb{P}\Big(\frac{r_i}{r_{i+1}} \leq x\Big)\mathbb{P}\Big(\frac{r_{i+1}}{r_{i+2}} \leq y\Big),\end{aligned}$$

where (a) follows from the fact that for Poisson point processes, r_{i+2} is independent of r_i given r_{i+1}. (b) follows from the independence of t_i and r_{i+1} as established in the proof of Lemma 1.

For $i + 1 < j$,

$$\begin{aligned}&\mathbb{P}(t_i \leq x, t_j \leq y) \\ &\quad= \mathbb{E}\Big[\mathbb{P}\Big(\frac{r_i}{r_{i+1}} \leq x, \frac{r_j}{r_{j+1}} \leq y \;\Big|\; r_{i+1}, r_j\Big)\Big] \\ &\quad= \mathbb{E}\Big[\mathbb{P}\Big(\frac{r_i}{r_{i+1}} \leq x \;\Big|\; r_{i+1}\Big)\mathbb{P}\Big(\frac{r_j}{r_{j+1}} \leq y \;\Big|\; r_j\Big)\Big] \\ &\quad= \mathbb{P}\Big(\frac{r_i}{r_{i+1}} \leq x\Big)\mathbb{P}\Big(\frac{r_j}{r_{j+1}} \leq y\Big).\end{aligned}$$

For the second part of the lemma, the same conditional expectation method is used. □

Lemma 2 is a key result that helps simplify the analysis related to the relative distances in Poisson networks. For instance, it immediately follows that t_1 is independent of any subset of $\{t_i\}_{i\geq 2}$.

B. Separability of the SIR MD in Poisson Networks

Theorem 1 (Separability)**.** For any independent fading in Poisson networks, there exists a function g such that

$$\bar{F}_{P_{\mathrm{s}}}(\theta, x) = g(x)\theta^{-\delta}, \quad (\theta, x) \in \mathcal{D}, \quad (11)$$

where

$$\mathcal{D} \triangleq \{(\theta, x)\colon \mathbb{P}(h_1/h_2 > \theta) \leq x\}, \quad (12)$$

and g depends on the statistics of all the fading random variables $\{h_i\}_{i\in\mathbb{N}}$. Further, g is monotonically decreasing from 0 to 1, with $g(1) = 0$, and for iid fading,

$$\int_0^1 g(x)\mathrm{d}x = \mathrm{sinc}(\delta). \quad (13)$$

Proof. First, we define the region $\mathcal{D}$ such that $P_{\rm s}(\theta)$ is a monotone decreasing function of t_1 regardless of $\{t_i\}_{i\geq 2}$. Specifically, we can write the conditional success probability as

$$P_{\rm s}(\theta) = \mathbb{P}\bigg(\frac{h_1 r_1^{-\alpha}}{\sum_{i=2}^{\infty} h_i r_i^{-\alpha}} > \theta \;\Big|\; \Phi\bigg) \tag{14}$$

$$= \mathbb{P}\bigg(\frac{h_1}{h_2} > \theta t_1^{\alpha}\Big(1 + \sum_{i=3}^{\infty} \frac{h_i r_2^{\alpha}}{h_2 r_i^{\alpha}}\Big) \;\Big|\; \Phi\bigg). \tag{15}$$

Letting $t_1 = 1$, we have

$$\mathbb{P}\bigg(\frac{h_1}{h_2} > \theta\Big(1 + \sum_{i=3}^{\infty} \frac{h_i r_2^{\alpha}}{h_2 r_i^{\alpha}}\Big) \;\Big|\; \Phi\bigg) \overset{\text{(a)}}{\leq} \mathbb{P}\bigg(\frac{h_1}{h_2} > \theta\bigg), \tag{16}$$

which follows from the fact that $\sum_{i=3}^{\infty} h_i r_2^{\alpha}/h_2 r_i^{\alpha} > 0$ almost surely. In $\mathcal{D}$, when $t_1 = 1$, the reliability cannot be higher than x regardless of $\{t_i\}_{i\geq 2}$. Thus, $P_{\rm s}(\theta)$ is a monotone decreasing function of t_1 in $\mathcal{D}$ regardless of $\{t_i\}_{i\geq 2}$. In other words, $P_{\rm s}(\theta) > x \Rightarrow t_1 < \rho_c$ for some $\rho_c \leq 1$.

Now, for $(\theta, x) \in \mathcal{D}$,

$$\begin{aligned}
\bar{F}_{P_{\rm s}}(\theta, x) &= \mathbb{P}(P_{\rm s}(\theta) > x) \\
&\overset{\text{(a)}}{=} \mathbb{P}(\theta t_1^{\alpha} < f(x, t_2^{\alpha}, ...)) \\
&= \mathbb{E}[\mathbb{P}(\theta t_1^{\alpha} < f(x, t_2^{\alpha}, ...) \mid t_2^{\alpha}, ...)] \\
&\overset{\text{(b)}}{=} \theta^{-\delta}\mathbb{E}[f(x, t_2, ...)^{\delta}] \\
&\overset{\text{(c)}}{=} \theta^{-\delta} g(x).
\end{aligned}$$

In step (a), we rewrite the conditional success probability such that f is a function of x and $\{t_i\}_{i\geq 2}$ by the definition of $\mathcal{D}$. Step (b) follows from the distribution of t_1 and its independence with $\{t_i\}_{i\geq 2}$. Step (c) follows from defining $g(x) \triangleq \mathbb{E}[f(x, t_2, ...)^{\delta}]$. $g(x)$ is a function of x determined by the fading statistic. g is monotonically decreasing from 0 to 1, with $g(1) = 0$ by the monotonicity of the MD in x and that $\bar{F}_{P_{\rm s}(\theta,1)} = 0$ for any θ.

For the second part, it is shown in [17, Theorem 4] that the success probability for the PPP with arbitrary iid fading satisfies

$$p_{\rm s}(\theta) \sim \operatorname{sinc}(\delta)\theta^{-\delta}, \quad \theta \to \infty. \tag{17}$$

Equivalently, $\lim_{\theta\to\infty} p_{\rm s}(\theta)\theta^{\delta} = \operatorname{sinc}(\delta)$. From the definition of the separable region,

$$\begin{aligned}
\int_0^1 g(x)\mathrm{d}x &= \int_0^1 \lim_{\theta\to\infty} \bar{F}_{P_{\rm s}}(\theta, x)\theta^{\delta}\mathrm{d}x \\
&= \lim_{\theta\to\infty} p_{\rm s}(\theta)\theta^{\delta} \\
&= \operatorname{sinc}(\delta).
\end{aligned}$$

Thus we obtain (13). □

Remark 1. Theorem 1 shows that in Poisson networks, the calculation of the SIR MD boils down to the CDF of t_1 due to the independence of t_1 with $\{t_i\}_{i\geq 2}$ and $\mathbb{P}(t_1 \leq \rho) = \rho^2$. The MD can be expressed as the product of two single-variable functions of x and θ. The region $\mathcal{D}$ depends on the fading statistics from two nearest BSs only, and the function f depends on all the fading statistics. Up to step (b), the derivation holds for general network models.

Remark 2 (Simulation of $g(x)$)**.** From (11), $g(x) = \bar{F}_{P_{\rm s}}(\theta, x)\theta^{\delta}$, $(\theta, x) \in \mathcal{D}$. The definition of $\mathcal{D}$ requires $\theta \to \infty$ to obtain the exact $g(x)$ for $x \in (0, 1]$. However, for a good approximation of $g(x)$, it suffices to simulate the SIR MD for a fixed and large θ, *e.g.*, $\theta = 100$. The simulation of the SIR MD for a fixed θ is straightforward. In cases where the analytical form of the conditional success probability is available (as, *e.g.*, for Rayleigh fading), only the distances $\{r_i\}_{i\in\mathbb{N}}$ need to be simulated.

Corollary 1. Let $\mathcal{D}$ be expressed in terms of $(1/(1+\theta), x) \subset [0, 1]^2$. For any iid fading, $\mathcal{D}$ always contains the point $(1/2, 1/2)$, and the area of $\mathcal{D}$ is 1/2.

Proof. The separable region $\mathcal{D}$ in terms of (θ, x) is given by (12) as

$$\begin{aligned}
x &\geq \mathbb{P}\left(h_1/h_2 > \theta\right) \\
&= \mathbb{P}\left(\frac{h_1 + h_2}{h_2} > \theta + 1\right) \\
&= \mathbb{P}\left(\frac{h_2}{h_1 + h_2} < \frac{1}{1 + \theta}\right).
\end{aligned}$$

Letting $t = 1/(1+\theta)$, we have $\mathcal{D} = \{(t, x)\colon x \geq \mathbb{P}(h_2/(h_1 + h_2) < t)\}$, which is a subset of $[0, 1]^2$. For any iid fading, $\mathbb{P}(h_2/(h_1 + h_2) < 1/2) = 1/2$. Thus $(1/2, 1/2) \in \mathcal{D}$.

The area of $\mathcal{D}$ is

$$\begin{aligned}
\int_{\mathcal{D}} \mathrm{d}x\mathrm{d}t &= \int_0^1 1 - \mathbb{P}\left(\frac{h_2}{h_1 + h_2} < t\right)\mathrm{d}t \\
&= 1 - \mathbb{E}\left[\frac{h_2}{h_1 + h_2}\right] \\
&\overset{\text{(a)}}{=} \frac{1}{2}.
\end{aligned}$$

Step (a) holds since $\mathbb{E}h_2/(h_1 + h_2) = \mathbb{E}h_1/(h_1 + h_2) = 1/2$ for any iid h_1, h_2. □

Remark 3. Corollary 1 shows that for any iid fading, $\mathcal{D}$ always covers half of the parameter space. Further, the boundary of $\mathcal{D}$, $x = \mathbb{P}(h_2/(h_1 + h_2) < t)$, is an odd function w.r.t. the center point $(1/2, 1/2)$. This is proved by showing that for iid fading,

$$\mathbb{P}(h_2/(h_1 + h_2) < t) + \mathbb{P}(h_2/(h_1 + h_2) < 1 - t) = 1.$$

C. Nakagami-m Fading

In this subsection, we study the separable region for iid Nakagami-m fading[3], $m > 0$. The rate of Nakagami-m fading is set to $1/m$ to have unit mean power for any m. We then focus on two special cases, namely no fading ($m \to \infty$) and Rayleigh fading ($m = 1$). Throughout the rest of the paper, we denote by h the fading random variable.

The PDF of Nakagami-m fading is

$$f_h(x) = \frac{m^m}{\Gamma(m)} x^{m-1} e^{-mx}, \quad x \geq 0, \tag{18}$$

[3]While Nakagami-m fading has been defined only for $m \geq 1/2$ [24], our results hold for any positive m.

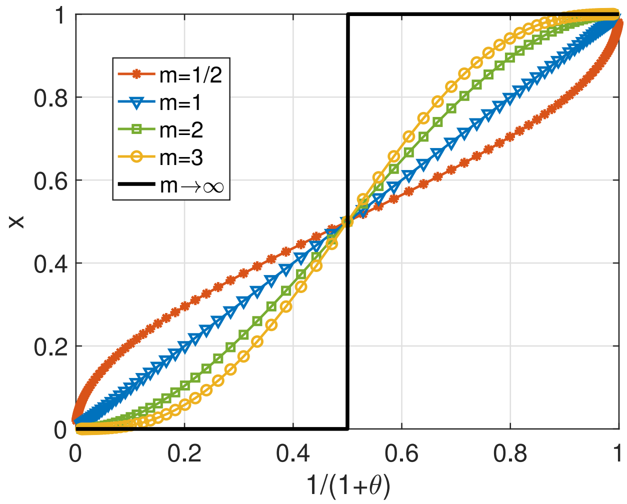

Fig. 3. The curve $x = I_{\frac{1}{1+\theta}}(m,m)$ (boundary of $\mathcal{D}$) versus $1/(1+\theta)$ for $m = 1/2, 1, 2, 3$, and $m \to \infty$.

and the CCDF is

$$\bar{F}_h(x) = \frac{m^m}{\Gamma(m)} \int_x^\infty t^{m-1} e^{-mt} \mathrm{d}t = \frac{\Gamma(m, mx)}{\Gamma(m)}.$$

Theorem 2. For Poisson networks with Nakagami-m fading,

$$\mathcal{D} = \left\{(\theta, x)\colon I_{\frac{1}{1+\theta}}(m,m) \le x\right\}, \tag{19}$$

where $\theta > 0, x \in [0,1]$, and $I_p(a,b)$ is the regularized incomplete beta function.

Proof.

$$\begin{aligned}
&\mathbb{P}(h_1/h_2 > \theta) \\
&\quad = \mathbb{E}\big[\mathbb{P}(h_1 > \theta h_2 \mid h_2)\big] \\
&\quad \overset{\text{(a)}}{=} \frac{1}{\Gamma(m)} \mathbb{E} \int_{m\theta h}^\infty t^{m-1} e^{-t} \mathrm{d}t \\
&\quad \overset{\text{(b)}}{=} \frac{m^m}{\Gamma(m)} \int_\theta^\infty \mathbb{E}\big[h^m e^{-mhu}\big] u^{m-1} \mathrm{d}u \\
&\quad \overset{\text{(c)}}{=} \frac{\Gamma(2m)}{(\Gamma(m))^2} \int_\theta^\infty \frac{1}{(1+u)^{m+1}} \frac{u^{m-1}}{(1+u)^{m-1}} \mathrm{d}u \\
&\quad \overset{\text{(d)}}{=} \frac{\int_0^{\frac{1}{1+\theta}} v^{m-1}(1-v)^{m-1} \mathrm{d}v}{B(m,m)} \\
&\quad = I_{\frac{1}{1+\theta}}(m,m).
\end{aligned}$$

Step (a) follows from the PDF of h. Step (b) follows from change of variable $u = t/mh$. Step (c) follows from $\mathbb{E}[h^m e^{-mhu}] = m^{-m}\Gamma(2m)/\Gamma(m)(1+u)^{2m}$ and (d) follows from change of variable $v = 1/(1+u)$. The last step follows from the definition of the regularized incomplete beta function. Letting $\mathbb{P}(h_1/h_2 > \theta) \le x$, we obtain $\mathcal{D}$. □

Fig. 3 shows the boundary of the separable region. We plot $I_{\frac{1}{1+\theta}}(m,m)$ versus $1/(1+\theta)$ for $m = 1/2,\ 1,\ 2,\ 3$, and $m \to \infty$. The x-axis is chosen such that it is in $[0,1)$. Note that the boundary $I_{\frac{1}{1+\theta}}(m,m)$ contains the point $(1/(1+\theta), x) = (1/2, 1/2)$ for any finite m, which is stated in Corollary 1. And the area of $\mathcal{D}$ is 1/2. For $m \to \infty$, $I_{\frac{1}{1+\theta}}(m,m)$ is a step function: $x = 1$ for $\theta < 1$, and $x = 0$ for $\theta \ge 1$. For $m \to 0$, $I_{\frac{1}{1+\theta}}(m,m) \to 1/2$ for any $\theta > 0$.

Now we consider two specific fading models: no fading and Rayleigh fading. The study of the no fading case offers insights on the impact of fading in the asymptotic scenario, which we will show later in Section IV.

1) No fading ($h \equiv 1$): Without fading, a link either always succeeds or always fails. The conditional success probability is

$$P_{\mathrm{s}}(\theta) = \begin{cases} 1, & r_1^{-\alpha}/\sum_{i=2}^\infty r_i^{-\alpha} > \theta \\ 0, & r_1^{-\alpha}/\sum_{i=2}^\infty r_i^{-\alpha} \le \theta, \end{cases} \tag{20}$$

and the MD follows as

$$\bar{F}_{P_{\mathrm{s}}}(\theta, x) = \begin{cases} \mathbb{P}(r_1^{-\alpha}/\sum_{i=2}^\infty r_i^{-\alpha} > \theta), & x \in [0,1) \\ 0, \quad x = 1. \end{cases} \tag{21}$$

Observe that $\mathbb{P}(r_1^{-\alpha}/\sum_{i=2}^\infty r_i^{-\alpha} > \theta)$ is the also the mean success probability for no fading. In other words, $\bar{F}_{P_{\mathrm{s}}}(\theta, x) \equiv p_{\mathrm{s}}(\theta)$ for $x \in [0,1)$.

Corollary 2. For Poisson networks with no fading,

$$\mathcal{D} = \{\theta \ge 1, x \in [0,1)\}. \tag{22}$$

Proof. Follows from Theorem 2 and $m \to \infty$. □

The boundary of $\mathcal{D}$ for this case is the black step function in Fig. 3.

Corollary 3. For Poisson networks with no fading,

$$g(x) \equiv \mathrm{sinc}(\delta). \tag{23}$$

Proof.

$$\mathbb{P}\left(\frac{r_1^{-\alpha}}{\sum_{i=2}^\infty r_i^{-\alpha}} > \theta\right) = \mathbb{P}\left(\theta t_1^\alpha < \left(\sum_{i=2}^\infty \left(\frac{r_2}{r_i}\right)^\alpha\right)^{-1}\right) \overset{\text{(a)}}{=} \theta^{-\delta}\mathbb{E}\left[\left(\sum_{i=2}^\infty \left(\frac{r_2}{r_i}\right)^\alpha\right)^{-\delta}\right],\ \theta \ge 1.$$

Step (a) follows from Corollary 2. Thus in this case, $f(x, t_2, t_3, \ldots) = (\sum_{i=2}^\infty (r_2/r_i)^\alpha)^{-1}$ and $g(x) = \mathbb{E}[(\sum_{i=2}^\infty (r_2/r_i)^\alpha)^{-\delta}]$.

We now use the probability generating functional (PGFL) of the PPP to calculate $g(x)$. First, for a random variable X

$$X^{-\delta} \equiv \frac{1}{\Gamma(\delta)} \int_0^\infty e^{-sX} s^{\delta-1} \mathrm{d}s \tag{24}$$

and

$$\mathbb{E}[X^{-\delta}] = \frac{1}{\Gamma(\delta)} \int_0^\infty \mathcal{L}_X(s) s^{\delta-1} \mathrm{d}s, \tag{25}$$

where $\mathcal{L}_X(s)$ is the Laplace transform of X. It is straightforward to calculate the Laplace transform of $\sum_{i=2}^\infty (r_2/r_i)^\alpha$ using the PGFL of the PPP. It follows that

$$g(x) = \mathrm{sinc}(\delta). \tag{26}$$

□

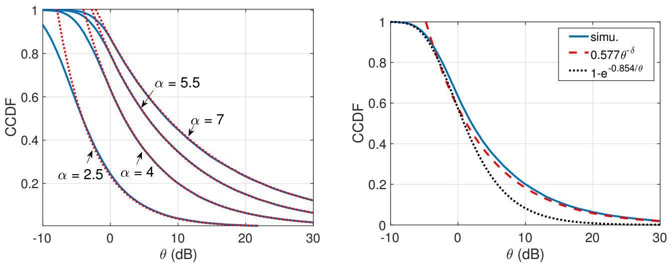

(a) Simulation (solid blue curves) and $\mathrm{sinc}(\delta)\theta^{-\delta}$ (dashed red curves), which are exact for $\theta \geq 1$, $\alpha = 2.5, 4, 5.5, 7$.

(b) Simulation, (27), and the asymptotic result as $\theta \to 0$ in [26, Theorem 1], $\alpha = 4$.

Fig. 4. SIR MD without fading for $x \in [0, 1)$.

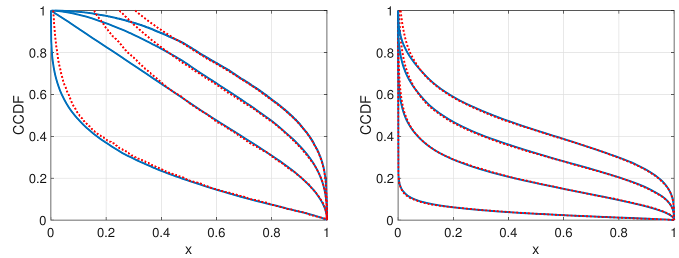

(a) $\theta = 1$. The separable region is $x \geq 0.5$.

(b) $\theta = 10$. The separable region is $x \geq 0.091$.

Fig. 5. Simulation of the SIR MD for Rayleigh fading (solid blue curves) and $g(x)\theta^{-\delta}$ (dashed red curves) for $\theta = 1$ and 10. The curves from lower left to upper right are results for $\alpha = 2.5, 4, 5.5, 7$, respectively.

Remark 4. The result of the mean success probability $p_{\mathrm{s}}(\theta) = \mathrm{sinc}(\delta)\theta^{-\delta}$ for $\theta \geq 1$ has been derived using different techniques in [20], [25] with different levels of generality, though not in the context of the SIR MD. It is shown in [20] that $p_{\mathrm{s}}(\theta) = \mathrm{sinc}(\delta)\theta^{-\delta}$ holds for the maximum instantaneous signal association for any iid fading including no fading. Further, in [26], an asymptotic form $p_{\mathrm{s}}(\theta) \sim 1 - \exp(s^*/\theta),\ \theta \to 0$ for no fading is derived. The value of s^* depends on α. For instance, $s^* = -0.854$ for $\alpha = 4$.

We now provide a simple lower bound for $g(x)$. By the convexity of $f(x) = x^{-\delta}$,

$$\mathbb{E}\Bigg[\bigg(\sum_{i=2}^{\infty}\Big(\frac{r_2}{r_i}\Big)^{\alpha}\bigg)^{-\delta}\Bigg] \geq \mathbb{E}\Bigg[\bigg(\sum_{i=2}^{\infty}\Big(\frac{r_2}{r_i}\Big)^{\alpha}\bigg)\Bigg]^{-\delta} \stackrel{\text{(a)}}{=} \Big(\frac{\alpha+2}{\alpha-2}\Big)^{-\delta},$$

where step (a) is calculated from the mean interference-to-signal ratio (MISR) in [27]. Thus we obtain a lower bound for the success probability

$$p_{\mathrm{s}}(\theta) \geq \theta^{-\delta}\Big(\frac{1+\delta}{1-\delta}\Big)^{-\delta}, \quad \theta \geq 1. \tag{27}$$

For $\alpha = 4$ $(\delta = 1/2)$, $p_{\mathrm{s}}(\theta) \geq \theta^{-\delta}/\sqrt{3} \approx 0.577\theta^{-\delta}$.

Fig. 4a shows the simulation result of the success probability for path loss exponents $\alpha = 2.5, 4, 5.5, 7$, which overlaps with $\mathrm{sinc}(\delta)\theta^{-\delta}$ for $\theta \geq 1$. Fig. 4b compares the approximation (27), the asymptotic result $p_{\mathrm{s}}(\theta) \sim 1 - e^{-0.854/\theta},\ \theta \to 0$ in [26, Theorem 1], and the simulation result.

2) Rayleigh fading: For Rayleigh fading, the conditional success probability is

$$P_{\mathrm{s}}(\theta) = \prod_{i=2}^{\infty}\frac{1}{1+\theta(r_1/r_i)^{\alpha}}. \tag{28}$$

Hence, only the distances need to be simulated to obtain the SIR MD.

Corollary 4. For Poisson networks with iid Rayleigh fading,

$$\mathcal{D} = \{(\theta, x) \colon 1 + \theta \geq x^{-1}\}. \tag{29}$$

Proof. From Theorem 2, we obtain $\mathcal{D}$ by letting $m = 1$. □

Simulation of $g(x)$: We simulate $\bar{F}_{P_{\mathrm{s}}}(100, x)$ and use $g(x) = \bar{F}_{P_{\mathrm{s}}}(100, x)100^{\delta}$ to obtain the exact $g(x)$ for $x \geq 0.0099$ and approximated g for $x < 0.0099$. The SIR MD for Rayleigh fading can be easily simulated for any fixed θ using Eq. (28). Fig. 5 shows the simulation results of the SIR MD for $\theta = 1,\ 10$, and $g(x)\theta^{-\delta}$ for path loss exponents $\alpha = 2.5, 4, 5.5, 7$. The separable regions are $x \geq 0.5$ and $x \geq 0.091$, respectively. As for the simulation complexity, finding $g(x)$ for $\alpha = 4$ via $\bar{F}_{P_{\mathrm{s}}}(100, x)100^{\delta}$ takes only about 35s using Matlab on a standard computer, with 100,000 samples.

Approximations of $g(x)$: $g(x)$ for Poisson networks with iid Rayleigh fading can be approximated by

$$g_1(x) = 1.298\left(\cot\left(\frac{\pi x^{0.25}}{2}\right)\right)^{0.6}, \tag{30}$$

$$g_2(x) = -1.226\log\left(\frac{1}{\pi}\arccos\left(-2x^{0.5}+1\right)\right), \tag{31}$$

and

$$g_{\mathrm{beta}}(x) \triangleq \lim_{\theta\to\infty}\bar{F}_{\mathrm{beta}}(\theta, x)\theta^{\delta}. \tag{32}$$

$\bar{F}_{\mathrm{beta}}(\theta, x)$ denotes the beta distribution-based approximation of the SIR MD proposed in [1], which only involves the first two moments of $P_{\mathrm{s}}(\theta)$. $g_1,\ g_2$ are fitting curves obtained via Matlab's Curves Fitting App that have an integral of $\mathrm{sinc}(\delta)$.

Fig. 6 shows the simulation result of g, the three approximations, and their differences. For g_{beta}, we use $\bar{F}_{\mathrm{beta}}(\theta, x)\theta^{\delta}$ with $\theta = 100$ as an approximation. The x-axis is limited to $[0.0099, 1]$ so that $(\theta, x) \in \mathcal{D}$. From the figure, it is apparent that $g_1,\ g_2,\ g_{\mathrm{beta}}$ give quite accurate approximations for g.

D. General Networks

To study the SIR MD for more general networks, we focus on two specific networks that model the repulsion between BS locations: Ginibre networks [28]–[30] and triangular lattice networks. We assume iid Rayleigh fading. We are interested in showing that $g(x)\theta^{-\delta}$ serves as a good approximation for these networks. To that end, we simulate the SIR MD for $x = 0.9$ and $x = 0.99$. We show that when θ is chosen large enough, $g(x)\theta^{-\delta}$ is indeed a good approximation. The choice of the "large enough" θ depends on the reliability x.

As is mentioned in Section III-C, only the distances need to be simulated to obtain the SIR MD with Rayleigh fading.

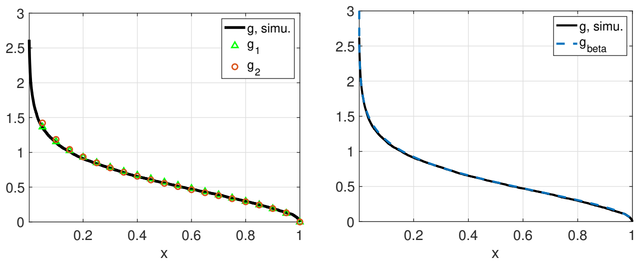

(a) $g(x)$ via simulation and g_1, g_2.

(b) $g(x)$ and its approximation using beta distribution.

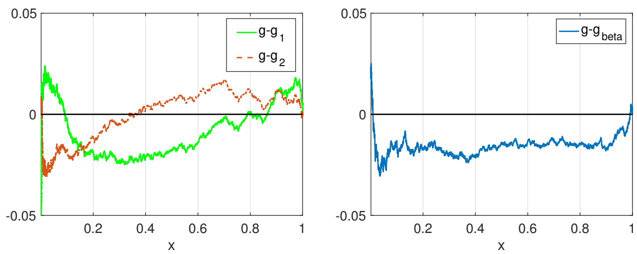

(c) Differences between g and g_1, g_2.

(d) Difference between g and g_{beta}.

Fig. 6. $g(x)$ via simulation, $g_1(x)$, $g_2(x)$, $g_{\text{beta}}(x)$, and their differences in Poisson networks with Rayleigh fading, $\alpha = 4$.

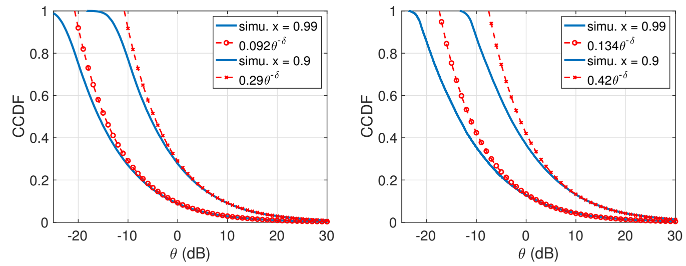

(a) Ginibre networks.

(b) Triangular lattice networks.

Fig. 7. Simulation and the $g(x)\theta^{-\delta}$ approximation of the SIR MD for $x = 0.9,\ 0.99$ in Ginibre networks and triangular lattice networks, Rayleigh fading, $\alpha = 4$.

The simulation of the distances in a triangular lattice network is straightforward. For Ginibre networks, we use the following proposition.

Proposition 1. [31, Proposition 4.3] The distances $\{r_i\}_{i\in\mathbb{N}}$, for a Ginibre point process have the same distribution as $\{\sqrt{Y_i}\}_{i\in\mathbb{N}}$, where $Y_i,\ i \in \mathbb{N}$, are mutually independent and Y_i follows the i-th Erlang distribution with unit-rate parameter[4], denoted by $Y_i \sim \Gamma(i, 1),\ i \in \mathbb{N}$.

Figs. 7a and 7b show the SIR MD in Ginibre networks and triangular lattice networks for $x = 0.9$ and $x = 0.99$. We consider $g(x)\theta^{-\delta}$ to be a good approximation when its relative error from the simulated result is less than 5%. For Ginibre networks, $0.29\theta^{-\delta}$ provides a good approximation for $\theta \geq 0$ dB when $x = 0.9$; the same accurateness holds with $0.092\theta^{-\delta}$ for $\theta \geq -6$ dB when $x = 0.99$. For triangular lattices, $0.42\theta^{-\delta}$ provides a good approximation for $\theta \geq 6$ dB when $x = 0.9$; the same accurateness holds with $0.134\theta^{-\delta}$ for $\theta \geq -1$ dB when $x = 0.99$. In comparison, for Poisson networks with Rayleigh fading, the "separable region" for $x = 0.9$ and $x = 0.99$ are $\theta \geq -9.54$ dB and $\theta \geq -20$ dB, respectively. Thus, $g(x)\theta^{-\delta}$ provides a good approximation for $\theta \geq -1$ dB when $x = 0.99$ in all cases studied.

IV. Asymptotics of the SIR MD in the Ultra-Reliable Regime

In this section, we focus on the asymptotics of the SIR MD as $x \to 1$ for general cellular networks with Rayleigh fading. We will show that the effect of the network geometry and Rayleigh fading are essentially separable when $x \to 1$.

[4]The intensity of this Ginibre point process is π^{-1}. Distances in a Ginibre point process with a different intensity can be obtained by scaling the rate parameter of the Erlang distribution.

A. General Networks

Lemma 3. [17, Theorem 4] For all simple stationary BS point processes Φ and iid fading[5] $\{h_x\}_{x\in\Phi}$, where the typical user is served by the nearest BS,

$$p_s(\theta) \sim C(\alpha)\theta^{-\delta}, \tag{33}$$

where[6]

$$C(\alpha) = \lambda\pi\mathbb{E}_o^!\Bigg[\bigg(\frac{h}{\sum_{x\in\Phi} h_x\|x\|^{-\alpha}}\bigg)^{\delta}\Bigg], \tag{34}$$

and $\mathbb{E}_o^!$ is the expectation with respect to the reduced Palm measure[7] of Φ.

Theorem 3. For all simple stationary point processes with Rayleigh fading, for any $x > 0$,

$$\bar{F}_{P_s}(\theta, x) = \Theta(\theta^{-\delta}), \quad \theta \to \infty, \tag{35}$$

and for any $\theta > 0$,

$$\bar{F}_{P_s}(\theta, x) \sim C(\alpha)(x^{-1} - 1)^{\delta}\theta^{-\delta}, \quad x \to 1, \tag{36}$$

where $C(\alpha)$ is defined in Lemma 3 with $h \equiv 1$.

Proof. For Rayleigh fading, the SIR MD is

$$\bar{F}_{P_s}(\theta, x) = \mathbb{P}\bigg(\prod_{i=2}^{\infty}\big(1 + \theta(r_1/r_i)^{\alpha}\big) < x^{-1}\bigg). \tag{37}$$

For $a_i > 0$, the inequalities

$$1 + \sum_i a_i \leq \prod_i (1 + a_i) \leq \exp\bigg(\sum_i a_i\bigg) \tag{38}$$

hold, and thus we can bound the SIR MD as

$$\mathbb{P}\bigg(\exp\bigg(\sum_{i=2}^{\infty}\theta\Big(\frac{r_1}{r_i}\Big)^{\alpha}\bigg) < x^{-1}\bigg) \leq \bar{F}_{P_s}(\theta, x)$$
$$\leq \mathbb{P}\bigg(1 + \sum_{i=2}^{\infty}\theta(r_1/r_i)^{\alpha} < x^{-1}\bigg).$$

[5] [19] derives a sufficient condition of Lemma 3 on the fading and the point process.

[6]There was a typo in the version published in the July 2020 issue of IEEE Transactions on Wireless Communication where $C(\alpha)$ was defined with an extra power of $1/\delta$ of the expectation in Eq (34). The typo is corrected in this manuscript.

[7]The reduced Palm distribution is the conditional point process distribution given that the typical point exists at a given location (the origin) but is excluded in the distribution [32, Chapter 8].

For the lower bound,

$$\mathbb{P}\bigg(\exp\bigg(\sum_{i=2}^{\infty}\theta\Big(\frac{r_1}{r_i}\Big)^{\alpha}\bigg)<\frac{1}{x}\bigg)=\mathbb{P}\bigg(\sum_{i=2}^{\infty}\theta\Big(\frac{r_1}{r_i}\Big)^{\alpha}<-\log x\bigg)$$

$$\sim C(\alpha)(-\log x)^{\delta}\theta^{-\delta}, \quad x\to 1, \tag{39}$$

$$\sim C(\alpha)(x^{-1}-1)^{\delta}\theta^{-\delta}, \quad x\to 1. \tag{40}$$

(39) also holds for any x and $\theta\to\infty$.

For the upper bound,

$$\mathbb{P}\bigg(1+\sum_{i=2}^{\infty}\theta\Big(\frac{r_1}{r_i}\Big)^{\alpha}<\frac{1}{x}\bigg)=\mathbb{P}\bigg(\sum_{i=2}^{\infty}\theta\Big(\frac{r_1}{r_i}\Big)^{\alpha}<\frac{1}{x}-1\bigg)$$

$$\sim C(\alpha)(x^{-1}-1)^{\delta}\theta^{-\delta}, \ x\to 1. \tag{41}$$

(41) also holds for any x and $\theta\to\infty$.

From (39) and (41), for any $x>0$, $\bar{F}_{P_s}(\theta,x)=\Theta(\theta^{-\delta})$, $\theta\to\infty$. For any $\theta>0$ and $x\to 1$, the asymptotic expressions (40) and (41) are the same, hence the proof is complete. □

Remark 5. Theorem 3 shows that the calculation of the MD in the limiting case boils down to the calculation of the SIR MD without fading. The effect of Rayleigh fading is captured by $(x^{-1}-1)^{\delta}$, and the effect of the network geometry is captured by $C(\alpha)$ (under no fading).

Remark 6. Taking the derivative of $g(x)$ at $x\to 1$ yields

$$\lim_{x\to 1}\frac{\partial \bar{F}_{P_s}(\theta,x)}{\partial x}=-\infty. \tag{42}$$

Given $F_{\bar{P}_s}(\theta,1)=0$, (42) implies that in the ultra-reliable regime, reducing the reliability requirement by a small amount leads to a significant increase of the user percentage satisfying the reliability requirement. This behavior is a result of the unboundedness of the power-law path loss and the distribution of t_1 as $t_1\to 0$. We contrast this result with that in Poisson bipolar networks [10] where

$$\lim_{x\to 1}\frac{\partial \bar{F}_{P_s}(\theta,x)}{\partial x}=0. \tag{43}$$

This follows from the derivative of $\bar{F}_{P_s}(\theta,x)\sim\exp(-C(1-x)^{-\delta/(1-\delta)})$, $x\to 1$, where $C=(\theta p\delta)^{\delta/(1-\delta)}(1-\delta)(\lambda\pi\Gamma(1-\delta))^{1/(1-\delta)}$ [10, Theorem 4]. Thus, the asymptotic behaviors of the MD for any θ as $x\to 1$ in cellular networks and Poisson bipolar networks are quite different. This is because in Poisson bipolar networks, the distance from the user to the desired transmitter is fixed, while in cellular networks, the user can be arbitrarily closer to the serving BS than to the interfering ones.

B. Poisson Networks

Corollary 5. For Poisson networks with Rayleigh fading, for any $\theta>0$ and $x\to 1$,

$$\bar{F}_{P_s}(\theta,x)\sim \operatorname{sinc}(\delta)\theta^{-\delta}(x^{-1}-1)^{\delta}. \tag{44}$$

Proof. It follows from Corollary 2 that $C(\alpha)=\operatorname{sinc}(\delta)$. □

In Poisson networks, by the definition of the separable region, for any θ, $(\theta,x)\in\mathcal{D}$ when $x\to 1$. Thus, (44) is equivalent to $g(x)\sim\operatorname{sinc}(\delta)(x^{-1}-1)^{\delta}$. Fig. 8 shows $g(x)$ from simulation and its asymptotic (44) for $\alpha=2.5,4,5.5,7$.

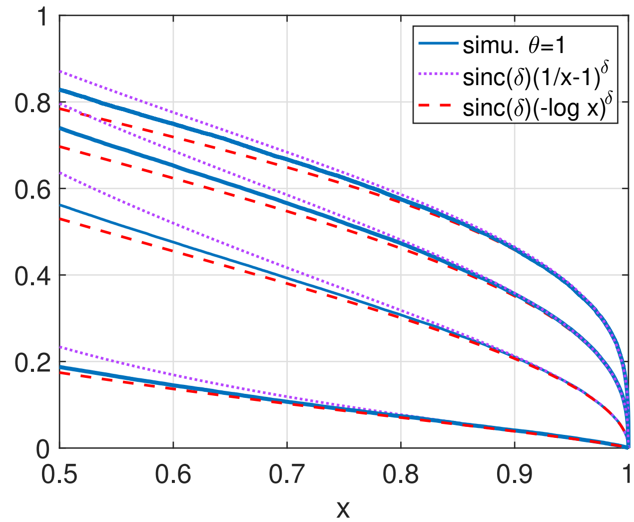

Fig. 8. $g(x)$ and its asymptotic form using (44) in Poisson networks with Rayleigh fading, $\alpha=2.5,4,5.5,7$ from lower left to upper right.

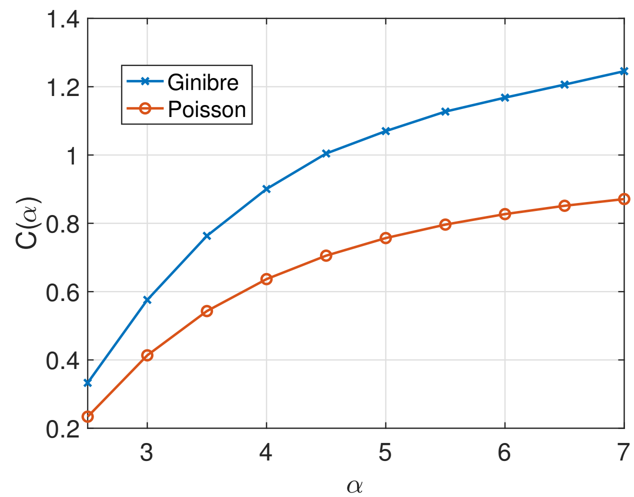

Fig. 9. $C(\alpha)$ for Poisson and Ginibre networks per (26) and (46).

C. Ginibre Networks

Proposition 2. [19, Proposition 3.1 (ii)] The distances $\{r_i\}_{i\in\mathbb{N}}$, for a Ginibre point process under the reduced Palm distribution, have the same distribution as $\{Y_{i+1}\}_{i\in\mathbb{N}}$, where $Y_i,\ i\in\mathbb{N}\setminus\{1\}$ are defined in Proposition 1.

Lemma 4. For Ginibre networks with no fading,

$$p_s(\theta)\sim C(\alpha)\theta^{-\delta}, \quad \theta\to\infty, \tag{45}$$

where

$$C(\alpha)=\mathbb{E}\bigg[\bigg(\sum_{i=2}^{\infty}Y_i^{-\frac{\alpha}{2}}\bigg)^{-\delta}\bigg] \tag{46}$$

and Y_i for $i\in\mathbb{N}\setminus\{1\}$, is defined in Proposition 1.

Proof. There are two ways to prove this lemma. The first is by directly applying Lemma 3, $h\equiv 1$, and the reduced Palm measure of Ginibre point processes given in Proposition 2. Alternatively, we can follow the proof for [18, Theorem 2] and replace Rayleigh fading with no fading. □

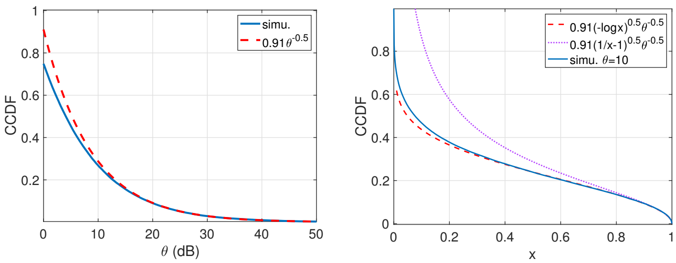

(a) The success probability with no fading.

(b) The SIR MD with Rayleigh fading.

Fig. 10. Asymptotic of the success probability for no fading as $\theta \to \infty$ and two bounds for the SIR MD in Ginibre networks with Rayleigh fading, $\alpha = 4$.

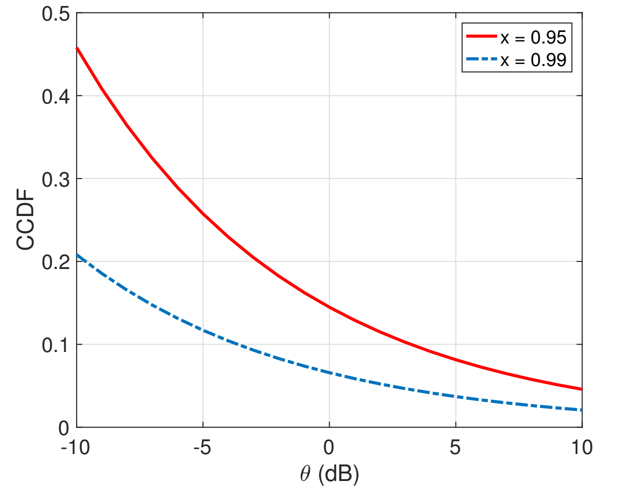

Fig. 11. Distribution of the SIR threshold $T(x)$ for reliability $x = 0.95$ and $x = 0.99$, Poisson networks, $\alpha = 4$.

Corollary 6. For Ginibre networks with Rayleigh fading,

$$\bar{F}_{P_s}(\theta, x) \sim C(\alpha)(x^{-1} - 1)^{\delta}\theta^{-\delta}, \quad x \to 1, \tag{47}$$

where $C(\alpha)$ is given in Lemma 4.

Proof. Follows directly from Theorem 3 and Lemma 4. □

Fig. 9 shows $C(\alpha)$ in Poisson and Ginibre networks for $\alpha \in [2.5, 7]$. The former has an explicit form $C(\alpha) = \text{sinc}(\delta)$ (see also (26)) and the latter is simulated using (46). For Ginibre networks and $C(4) \approx 0.91$. Fig. 10 shows the result in Lemma 4 and the two bounds (39) and (41). Note that from Fig. 10b, the lower bound (39) is much tighter than the upper bound.

V. Other Applications of the SIR MD

The link reliability, rate, and latency in wireless networks are fundamentally intertwined. In this section, we apply the results of the SIR MD to study the distribution of the link rate and local delay. It is shown in [15, Theorem 1] that the MD can be interpreted as the distribution of the SIR threshold for a fixed link reliability x, denoted by $T(x)$. In adaptive transmission techniques, based on the channel quality of each link, the transmission rate (modulation and coding scheme) is chosen such that a certain reliability can be achieved. For instance, in a network where the target reliability $x = 0.99$, the SIR threshold at each individual link is adjusted such that $\mathbb{P}(\text{SIR} > T(0.99) \mid \Phi) = 0.99$. The local delay is defined as the number of transmissions needed for a message to be received successfully. Retransmissions are less likely to occur for links with a high reliability. The distribution of the delay and, especially, its tail, is a critical metric in 5G cellular networks and beyond. We focus on Poisson networks with Rayleigh fading.

A. Rate

The distribution of the SIR threshold determines the distribution of the transmission rate by the Shannon formula. The normalized rate in nats/Hz/s for a given reliability is defined as

$$\mathcal{R} \triangleq x \log(1 + T(x)), \tag{48}$$

where $T(x)$ is the SIR threshold that satisfies the reliability x. It is a random variable whose distribution is a function of x. Let $\bar{\mathcal{R}} \triangleq \mathbb{E}[\mathcal{R}]$ be the ergodic rate for a given reliability x. There is a trade-off between the reliability and the ergodic rate. Setting $x \to 0$ or $x \to 1$ will result in arbitrarily small rate, either due to an ultra-low reliability or due to an ultra-low SIR threshold. Hence, there is an optimal reliability $0 < x < 1$ that maximizes the ergodic rate.

Fig. 11 shows the distribution of the SIR threshold when the reliability in the network is fixed. From Theorem 1, when $(\theta, x) \in \mathcal{D}$, the two curves only differ in the constant ratio $0.99g(0.99)/0.95g(0.95) \approx 0.47$, where $g(0.95) = 0.1448$ and $g(0.99) = 0.0658$ are obtained through simulation.

Corollary 7. In Poisson networks, the rate distribution satisfies

$$\bar{F}_{\mathcal{R}}(r) = g(x)(e^{r/x} - 1)^{-\delta}, \quad (e^{r/x} - 1, x) \in \mathcal{D}. \tag{49}$$

and the ergodic rate satisfies

$$\bar{\mathcal{R}} \sim \frac{\pi}{\sin(\pi\delta)} x g(x), \quad x \to 1. \tag{50}$$

Proof. For a given reliability x, the rate distribution can be written in the form of the SIR MD as $\bar{F}_{\mathcal{R}}(r) = \bar{F}_{P_s}(e^{r/x} - 1, x)$ [15]. Hence,

$$\bar{F}_{\mathcal{R}}(r) = g(x)(e^{r/x} - 1)^{-\delta}, \quad (e^{r/x} - 1, x) \in \mathcal{D}, \tag{51}$$

which follows from Theorem 1. Solving $e^{r/x} - 1 \geq \frac{1}{x} - 1$ for r for a given x using the definition of $\mathcal{D}$ yields $r \geq -x \log x$. The ergodic rate for a given reliability x is

$$\begin{aligned}\bar{\mathcal{R}} &= \int_0^{-x\log x} \bar{F}_{\mathcal{R}}(r)\mathrm{d}r + g(x)\int_{-x\log x}^{\infty} (e^{r/x} - 1)^{-\delta}\mathrm{d}r \\ &= \int_0^{-x\log x} \bar{F}_{\mathcal{R}}(r)\mathrm{d}r + xg(x)\int_{-\log x}^{\infty} (e^{t} - 1)^{-\delta}\mathrm{d}t.\end{aligned} \tag{52}$$

The first integral approaches 0 as $x \to 1$ faster than the second integral since $g(x) \sim (x^{-1} - 1)^{\delta}$, and so

$$\bar{\mathcal{R}} \sim xg(x)\int_0^{\infty} (e^{t} - 1)^{-\delta}\mathrm{d}t, \quad x \to 1, \tag{53}$$

which evaluates to (50). □

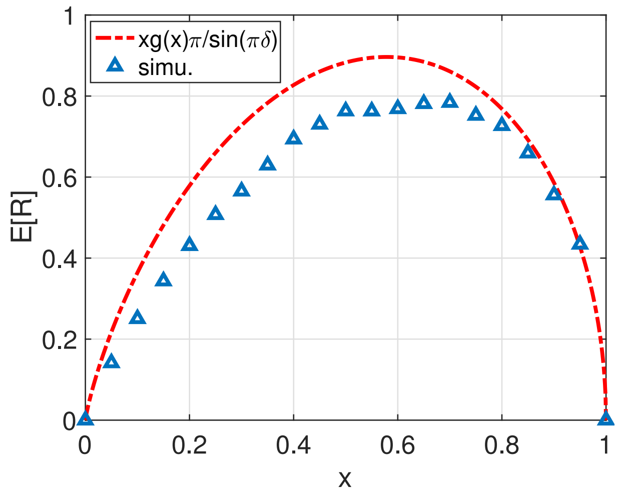

Fig. 12. The average rate $\bar{\mathcal{R}}$ and its approximation per (53) versus the reliability x.

With rate adaptation, the ergodic rate is a function of the target reliability. Fig. 12 plots the trade-off of the ergodic rate versus the reliability x per Corollary 7. $g(x)$ is simulated as in Section III C-2. (50) is asymptotically exact as $x \to 1$. It provides an upper bound for $\bar{\mathcal{R}}$ in general and an accurate approximation when $x \geq 0.8$. It is worth noting that in the simulated per-link rate-reliability trade-off, the optimum rate $\bar{\mathcal{R}} \approx 0.8$ [nats/s/Hz] is achieved at some point for $x \in [0.65, 0.75]$.

B. Local Delay

The local delay is defined as the number of transmissions, averaged over the fading, needed for a message to be received successfully. Denote by $D(\theta)$ the local delay as a function of θ. We have $D(\theta) \equiv 1/P_{\mathrm{s}}(\theta)$ (the mean of a geometric distribution with success probability $P_{\mathrm{s}}(\theta)$). In other words, the local delay for any individual link is the multiplicative inverse of the link reliability $P_{\mathrm{s}}(\theta)$. It is known that the mean local delay $\mathbb{E}[D(\theta)] = (1-\delta)/(1-\delta(1+\theta))$ for $\theta < 1/\delta - 1$ in Poisson networks with Rayleigh fading [1, Theorem 2]. Here, we provide the asymptotic form of the CDF of the local delay.

Lemma 5. The CDF of the local delay in the network can be expressed using the SIR meta distribution as

$$\mathbb{P}(D(\theta) \leq t) = \bar{F}_{P_{\mathrm{s}}}(\theta, t^{-1}), \quad t \geq 1. \tag{54}$$

Proof. Rewriting the CDF of the local delay as $\mathbb{P}(D(\theta) \leq t) = \mathbb{P}(P_{\mathrm{s}}(\theta) \geq t^{-1})$ we obtain (54). □

Corollary 8. For Poisson networks with Rayleigh fading,

$$\mathbb{P}(D(\theta) \leq 1+\epsilon) = g\big((1+\epsilon)^{-1}\big)\theta^{-\delta}, \quad \theta \geq \epsilon. \tag{55}$$

And for any $\theta > 0$,

$$\mathbb{P}(D(\theta) \leq 1+\epsilon) \sim \operatorname{sinc}\delta\epsilon^{\delta}\theta^{-\delta}, \quad \epsilon \to 0. \tag{56}$$

Proof. Let $\epsilon \triangleq t-1$. The results follow directly from Theorem 1, Theorem 2 and Lemma 4. □

Eq. (56) shows the trade-off between the SIR threshold and the target local delay. Note that by Theorem 3, the distribution across different types of network models (satisfying the condition in Theorem 3) only differs in a constant ratio. Essentially, the fraction of links satisfying a mean local delay constraint w.r.t. θ only depends on the ratio ϵ/θ. For more general networks, the constant $\operatorname{sinc}(\delta)$ is replaced by $C(\alpha)$, which is defined as in Lemma 4.

VI. Conclusions

In this work, we focus on the analytical properties of the SIR MD and their applications in cellular networks. We show that in Poisson networks with independent fading and power-law path loss with exponent α, the SIR MD can be written in the form of $g(x)\theta^{-2/\alpha}$ in a separable region. The separable region covers half of the unit square when expressed in terms of $(1/(1+\theta), x) \subset [0,1]^2$. We show that in Ginibre and triangular lattice networks, $g(x)\theta^{-2/\alpha}$ provides a good approximation. Specifically, its relative error with simulation results is less than 5% percent for $\theta \geq -1$ dB when $x = 0.99$ in all cases studied. Further, we show that the asymptotic form of the SIR MD for general network models with Rayleigh fading depends on the asymptotic form of the success probability for no fading, which essentially separates the effect of the network geometry and fading. Finally, this work shows the applications of the SIR MD to characterize the distribution of the link rate and local delay, whose analyses are critical in ultra-reliable and low-latency communication systems. For further work, the methodology of analyzing the MD based on "local information" and separating the effect of fading and network geometry can be applied to more general scenarios, including models with noise and bounded/multi-slope path loss.

References

[1] M. Haenggi, "The meta distribution of the SIR in Poisson bipolar and cellular networks," *IEEE Transactions on Wireless Communications*, vol. 15, no. 4, pp. 2577–2589, Apr 2016.

[2] Q. Cui, X. Yu, Y. Wang, and M. Haenggi, "The SIR meta distribution in Poisson cellular networks with base station cooperation," *IEEE Transactions on Communications*, vol. 66, no. 3, pp. 1234–1249, Mar 2018.

[3] M. Salehi, H. Tabassum, and E. Hossain, "Meta distribution of SIR in large-scale uplink and downlink NOMA networks," *IEEE Transactions on Communications*, vol. 67, no. 4, pp. 3009–3025, Apr 2019.

[4] N. Deng and M. Haenggi, "SINR and rate meta distributions for HCNs with joint spectrum allocation and offloading," *IEEE Transactions on Communications*, vol. 67, no. 5, pp. 3709–3722, May 2019.

[5] Y. Wang, M. Haenggi, and Z. Tan, "SIR meta distribution of K-tier downlink heterogeneous cellular networks with cell range expansion," *IEEE Transactions on Communications*, vol. 67, no. 4, pp. 3069–3081, Apr 2019.

[6] ——, "The meta distribution of the SIR for cellular networks with power control," *IEEE Transactions on Communications*, vol. 66, no. 4, pp. 1745–1757, Apr 2018.

[7] P. D. Mankar, H. S. Dhillon, and M. Haenggi, "Meta distribution analysis of the downlink SIR for the typical cell in a Poisson cellular network," in *IEEE Globecom*, 2019.

[8] S. S. Kalamkar and M. Haenggi, "Simple approximations of the SIR meta distribution in general cellular networks," *IEEE Transactions on Communications*, vol. 67, no. 6, pp. 4393–4406, Jun 2019.

[9] S. Wang and M. Di Renzo, "On the meta distribution in spatially correlated non-Poisson cellular networks," *EURASIP Journal on Wireless Communications and Networking*, no. 161, Jun 2019.

[10] S. S. Kalamkar and M. Haenggi, “The spatial outage capacity of wireless networks,” *IEEE Transactions on Wireless Communications*, vol. 17, no. 6, pp. 3709–3722, Jun 2018.

[11] A. P. Kartun-Giles, K. Koufos, and S. Kim, “Meta distribution of SIR in ultra-dense networks with bipartite Euclidean matchings,” *arXiv preprint arXiv:1910.13216*, 2019.

[12] M. Haenggi, “Efficient calculation of meta distributions and the performance of user percentiles,” *IEEE Wireless Communications Letters*, vol. 7, no. 6, pp. 982–985, Dec 2018.

[13] S. Guruacharya and E. Hossain, “Approximation of meta distribution and its moments for Poisson cellular networks,” *IEEE Wireless Communications Letters*, vol. 7, no. 6, pp. 1074–1077, Dec 2018.

[14] K. Feng and M. Haenggi, “On the location-dependent SIR gain in cellular networks,” *IEEE Wireless Communications Letters*, vol. 8, no. 3, pp. 777–780, Jun 2019.

[15] S. S. Kalamkar and M. Haenggi, “Per-link reliability and rate control: Two facets of the SIR meta distribution,” *IEEE Wireless Communications Letters*, vol. 8, no. 4, pp. 1244–1247, Aug 2019.

[16] M. Bennis, M. Debbah, and H. V. Poor, “Ultrareliable and low-latency wireless communication: Tail, risk, and scale,” *Proceedings of the IEEE*, vol. 106, no. 10, pp. 1834–1853, Oct 2018.

[17] R. K. Ganti and M. Haenggi, “Asymptotics and approximation of the SIR distribution in general cellular networks,” *IEEE Transactions on Wireless Communications*, vol. 15, no. 3, pp. 2130–2143, Mar 2016.

[18] N. Miyoshi and T. Shirai, “A cellular network model with Ginibre configured base stations,” *Advances in Applied Probability*, vol. 46, no. 3, pp. 832–845, 2014.

[19] ——, “Tail asymptotics of signal-to-interference ratio distribution in spatial cellular network models,” *Probability and Mathematical Statistics*, vol. 37, no. 2, pp. 431–453, Jan 2017.

[20] X. Zhang and M. Haenggi, “The performance of successive interference cancellation in random wireless networks,” *IEEE Transactions on Information Theory*, vol. 60, no. 10, pp. 6368–6388, Oct 2014.

[21] M. Haenggi, “The local delay in Poisson networks,” *IEEE Transactions on Information Theory*, vol. 59, no. 3, pp. 1788–1802, Mar 2013.

[22] S. Weber, “The value of observations in predicting transmission success in wireless networks under slotted Aloha,” in *2017 15th International Symposium on Modeling and Optimization in Mobile, Ad Hoc, and Wireless Networks (WiOpt)*, May 2017, pp. 1–8.

[23] M. Haenggi, “On distances in uniformly random networks,” *IEEE Transactions on Information Theory*, vol. 51, no. 10, pp. 3584–3586, Oct 2005.

[24] M. Nakagami, “The m-distribution—a general formula of intensity distribution of rapid fading,” in *Statistical Methods in Radio Wave Propagation*. Pergamon, 1960, pp. 3 – 36.

[25] H. S. Dhillon, R. K. Ganti, F. Baccelli, and J. G. Andrews, “Modeling and analysis of K-tier downlink heterogeneous cellular networks,” *IEEE Journal on Selected Areas in Communications*, vol. 30, no. 3, pp. 550–560, Apr 2012.

[26] R. K. Ganti and M. Haenggi, “SIR asymptotics in Poisson cellular networks without fading and with partial fading,” in *2016 IEEE International Conference on Communications (ICC)*, May 2016, pp. 1–5.

[27] M. Haenggi, “The mean interference-to-signal ratio and its key role in cellular and amorphous networks,” *IEEE Wireless Communications Letters*, vol. 3, no. 6, pp. 597–600, Dec 2014.

[28] J. Ginibre, “Statistical ensembles of complex, quaternion, and real matrices,” *Journal of Mathematical Physics*, vol. 6, no. 3, pp. 440–449, 1965.

[29] O. Macchi, “The coincidence approach to stochastic point processes,” *Advances in Applied Probability*, vol. 7, no. 1, pp. 83–122, 1975.

[30] N. Deng, W. Zhou, and M. Haenggi, “The Ginibre point process as a model for wireless networks with repulsion,” *IEEE Transactions on Wireless Communications*, vol. 14, no. 1, pp. 107–121, Jan 2015.

[31] L. Decreusefond, I. Flint, and A. Vergne, “A note on the simulation of the Ginibre point process,” *Journal of Applied Probability*, vol. 52, no. 4, pp. 1003–1012, 2015.

[32] M. Haenggi, *Stochastic geometry for wireless networks*. Cambridge University Press, 2012.